Compact Folded-Shorted Patch Antenna Array with PCB Implementation for Modern Small Satellites

Yuepei Li
Institute of Sensors, Signals & Systems,
Heriot Watt University,
Edinburgh, UK
yl12@hw.ac.uk

Symon K. Podilchak
Institute of Digital Comms.,
University of Edinburgh,
Edinburgh, UK
s.podilchak@ed.ac.uk

Dimitris E. Anagnostou
Institute of Sensors, Signals & Systems,
Heriot Watt University,
Edinburgh, UK
d.anagnostou@hw.ac.uk

***Abstract*—A compact circularly polarized (CP) antenna array is presented. The array utilizes folded-shorted patches (FSPs) and printed circuit board (PCB) technology for antenna miniaturization. Both techniques enable a size decrease of the quarter-wavelength shorted-patch by a factor of 1/N, where N is number of the layers above the ground plane while maintaining a quarter-wavelength resonant length. This results in a reduction of the antenna length by half or more. The feature of CP is achieved by a compact and planar feeding circuit defined by a network of meandered 90 and 180-degree hybrid couplers which can provide quadrature feeding of the FSP elements and can be integrated onto the backside of the antenna ground plane which is only 9 cm × 9 cm. To fine tune the resonant frequency of the FSP antenna, we select different relative permittivity values for the substrate. Agreement in terms of the simulations and measurements is observed for the compact antenna (size of 0.129λ × 0.129λ × 0.014λ) with realized gain, radiation beam patterns and axial ratio values reported at UHF frequencies (430 MHz).**

TABLE OF CONTENTS

1. INTRODUCTION

Modern small satellites (MSSs) are widely used and manufactured for earth observation and space telecommunications. The design, construction, testing and launching of satellites typically requires a large budget. When compared to large scale satellites, the MSS can significantly reduce launching costs, mission development time and make access to space more affordable [1]. Therefore, when considering microsatellite-to-microsatellite or microsatellite to ground station communications at UHF band frequencies, an antenna that is low profile, offers low cost fabrication, and with ease of installation is an attractive solution.

The conventional patch antenna is typically considered for other communication applications and has a standard resonant length λ/2 (where λ is the free-space wavelength defined in this paper). It can be used with a high relative permittivity ε_r value for the PCB substrate to reduce antenna size. The resonant length can be further reduced to λ/4 by introducing a shorting wall. Other techniques to reduce the size of patch antennas include reactive loading, slots and pins [2-5]. These approaches may be useful for microsatellites or smaller satellites. However, with antenna miniaturization, the bandwidth and the radiation efficiency can decrease, since these factors are related to the physical size of the antenna [6]. In [7], the authors initially presented the folded-shorted patch (FSP) antenna concept by proposing to fold both the patch and the ground plane into two layers, and in [8], such a linearly polarized multilayer FSP antenna was reported by increasing the number of layers. In that work the resonant frequency was set to 400 MHz, and lower frequencies as well, realizing a single-element size of 0.13λ × 0.14λ × 0.032λ.

Here we propose a new and highly compact multilayer layer FSP offering circular polarization (CP) using standard PCB technology and utilizing sequential rotation of four linearly polarized elements in a 2 × 2 array for use on CubeSats, microsatellites as well as other applications where compact antenna structures are required. The physical size of the single element is 0.056λ × 0.059λ × 0.015λ. The footprint of the FSP array is 0.133λ × 0.133λ when considering the UHF frequency band at 440 MHz (see Figs. 1 and 2). For this new antenna array design, the PCB material is placed in the region of the radiating patch edge and the second layer (see Fig. 2). This method can miniaturize the total array while maintaining the operating frequency and achieving maximum realized gain values of about 2 dBic, a good total antenna efficiency, and wide axial ratio beamwidth. Measurement results of such a multilayer FSP array are reported to validate the design. The simulations, assembly issues, and measurements are presented herein.

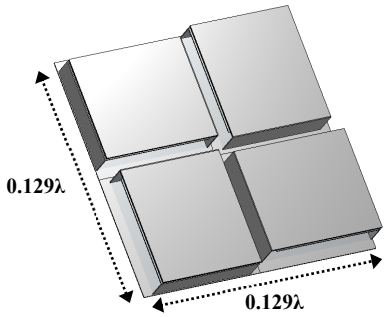

Fig. 1. Proposed UHF-band 2 × 2 antenna array for micro-satellites with sequentially rotated FSPs. Dimensions: 9 cm × 9 cm; operating frequency: 430 MHz.

2. Design Overview and Considerations For the Compact FSP Array

The configuration of the miniaturized, PCB implemented FSP antenna is shown in Fig. 2. The folding technique forces the fields to follow a meandered patch, enabling size reduction. As reported in the literature, fabrication and miniaturization can be achieved by using PCB technology. In [6], the multilayer FSP using PCB technology was initially presented, where the total structure was 0.2λ × 0.2λ × 0.05λ and the operating frequency was designed for 400 MHz. Maximum simulated realized gain values were about 2.5 dBic, but the measured realized gain was reduced to 0.5 dBic.

In this work a simpler method is employed by inserting a PCB substrate between the top and second layers only (see Fig. 2) which can miniaturize the total structure for a size of 0.129λ × 0.129λ × 0.014λ while still maintaining decent efficiency. The total antenna structure is 9 cm × 9 cm and thus suitable for CubeSats and other small satellites. When comparing these achievements to other works, two units of a 2 × 2 FSP array were implemented in [9] on a small satellite body with physical dimensions of 0.5 × 0.5 × 0.5 m^3 with an operating frequency of 400 MHz. In addition, that antenna can radiate in three operational modes by changing the sequentially rotated phase delay on each port connected to the antenna [9].

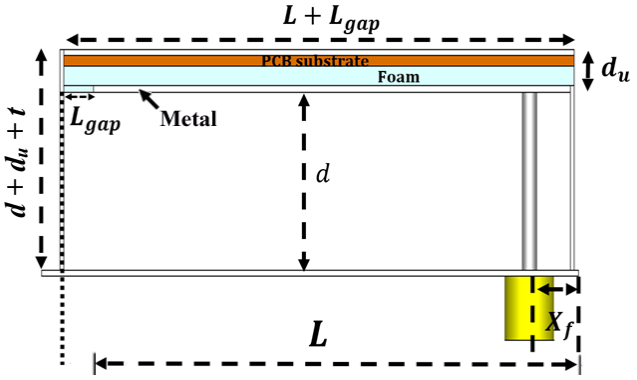

Fig. 2. Cross-section view of the single-element, two-layer FSP antenna (notice the L_{gap}) with dimensions: L_{gap} = 2.5 mm, $d_u = d_{substrate} + d_{foam}$ = 1.4 mm, L = 42.8 mm, W = 38 mm, metal thickness t = 0.3 mm, d = 8.3 mm, $d_{substrate}$ = 0.635 mm, d_{form} = 0.765 mm and X_f = 2.8 mm. The layers are defined at the height of $d + d_u + t$ and $d + t$, respectively. The material between the layers can be defined by the value of ε_r allowing for PCB or metallic-based implementation.

By following these developments, we propose in this work a compact 9 × 9 × 1 cm^3 FSP 2×2 antenna array (see Fig. 1) and supporting feeding system for CP operation at about 430 MHz. The feeding system can be integrated on the underside of the antenna array which can provide the needed sequentially rotated phase shifts for left-handed circular polarization (LHCP) radiation. These phase shifts are achieved by an integrated feeding network defined by two 90° and one 180° hybrid couplers using transmission line meandering for compactness. In addition, the feeding system and the FSP array have the same total structure size of 9 cm × 9 cm. Also, the FSP layer lengths and widths can be determined using transmission line theory by following [6] and [10].

Single-Element and Array Design

The proposed FSP antenna element has been designed using a shorting wall with PCB loading. Two substrate materials have been used; i.e. a low dielectric constant substrate Roger RT5880 (ε_r = 2.2, tanδ = 0.0009) and a high dielectric constant substrate material Roger RT6010LM (ε_r = 10.2, tanδ = 0.0023). In addition, we have investigated the matching frequency and $|S_{11}|$ by changing the values of the dielectric substrate. The measured and simulated reflection coefficient of the FSP antenna array (element 1, when considering the array) is shown in Fig. 3.

The FSP antenna array was originally designed for 425 MHz. Measured dimensions of the fabricated prototype have been imported to the simulation software CST. Matching frequency minimums are shifted by roughly 3 MHz and all reflection coefficient values are around -10 dB. Also, the separation between the top and second layers was optimized for the required resonant frequency by adjusting the dimension d_u. This parameter has been varied in Fig. 3 where it is shown that the resonant frequency can be adjusted between about 320 MHz to 470 MHz. In this experiment we have employed the 0.635 mm thickness of the dielectric substrate RT6010 LM, by increasing the substrate thickness, the resonant frequency can be reduced (see Fig. 4). In addition, where d_u is the dimension of the substrate thickness $d_{substrate}$ and the foam thickness d_{foam}.

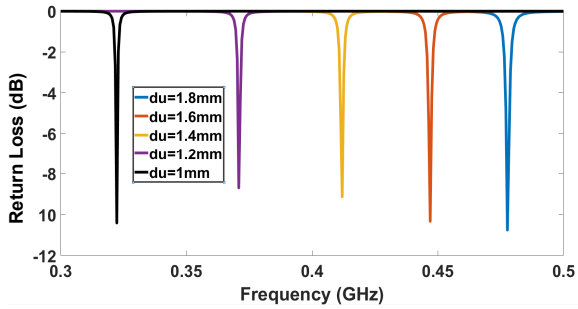

Fig. 3. Simulated $|S_{11}|$ showing the single element design frequency variation as compared to d_u; i.e. the height of the top layer above the first layer (see Fig. 2).

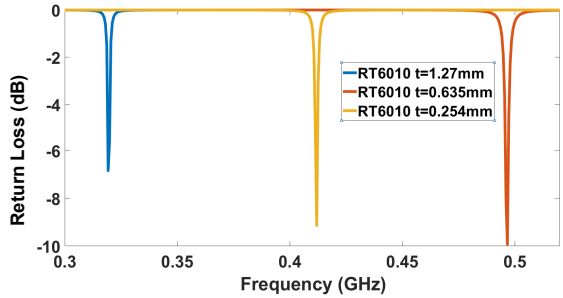

Fig. 4. Simulated $|S_{11}|$ showing the single element design frequency variation for a RT6010 LM substrate thickness $d_{substrate}$ being 0.254, 0.635 and 1.27 mm.

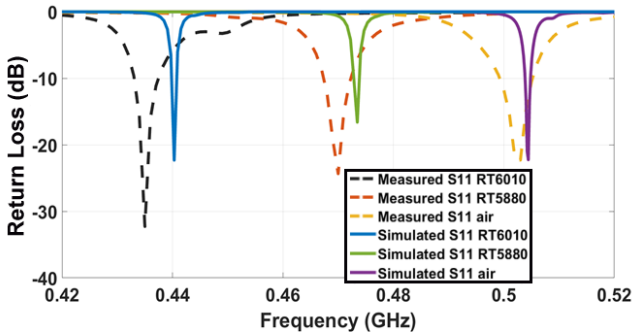

Fig. 5. Simulated and measured reflection coefficient $|S_{11}|$ for different dielectric constant values of the material.

The linearly polarized FSP antenna element was also designed considering lossy copper for all the required metal segments with a 0.3 mm thickness for the shorting wall as well as for the top and second layers. Also, 50-Ω coaxial probe feeding was employed for the individual element at an optimized position (see Fig. 5) for best matching and realized gain at 440 MHz considering the substrate RT6010 LM.

Generation of Circular Polarization

Each linearly polarized folded-shorted patch element on the ground plane, and a sequentially rotated array allows for the realization of CP radiation using linearly polarized elements [11]. In our system each antenna element within the sequentially rotated array is also fed with equal amplitude and a sequential phase shift. For example, in the most common configuration of a 2 × 2 array, each antenna (anti-clockwise rotation) is required to have a specific phase delay of 0°, 90°, 180° and 270°. This phase delay arrangement would generate LHCP. For right-handed circular polarization (RHCP), similar phase shifts would need to increase clockwise [11]. This technique can also reduce cross-polarization levels and improve the axial ratio bandwidth of the antenna. Further details of the employed feeding circuit can be found in the next sub-section.

Considering array theory, the larger the number of individual antenna elements used, the higher the antenna gain and the narrower the beam. Here we desire a compact antenna design with improved radiation performance, that also maintains a broad beam and a 2 × 2 array is proposed. However, this system configuration requires a feeding circuit using a multi-port combiner system that has to be bonded to the underside of the antenna ground plane to maintain its low-profile and compact features.

Feed System Design & Operation

The designed and fabricated feeding system shown in Fig. 6 is a 5-port network where each port provides the required 90° phase shift and equal power splitting. Also, the feeding system employed a high permittivity material RT6010 LM (ε_r = 10.2, tanδ = 0.0023, thickness = 0.4mm) while also using meandered microstrip sections to reduce physical dimensions. By following the operation of this feeding system, port 1 can be considered the input port, with port 2 providing a 270° phase delay, port 3 providing a +/-180° phase delay, port 4 providing a 90° phase delay, finally, port 5 provides a 360° or 0° phase delay. Therefore, the feeding system provides sequential phase rotation to generate LHCP radiation.

The highlighted numbers 1 and 3 (see Fig. 6) are the meandered 90° hybrid couplers where their physical dimensions have been reduced by 80% from the standard hybrid whilst considering the same substrate. The highlighted number 2, is the meandered rat-race coupler. Its physical dimensions have been reduced by 90%. Also, to conform to the dimensions of the array, the total physical dimension of the feeding system was also 9 cm x 9 cm. Measurement results for this feeding circuit suggest suitable performance; i.e. at the operating frequency of 430 MHz the required phase shifts are achieved and $|S_{11}| < -18$ dB, the output magnitude imbalance is 0.7dB and phase differences are -92.5°, -179°, 85°, 7°, respectively (see Figs. 7 and 8). Also, the average of the transmission coefficients was -7 dB which defines an average insertion loss of around 1.5 dB to 1.75 dB, which can be attributed to the value of tanδ for the employed substrate RT6010 LM.

The simulated realized gain for the 2×2 array with the far-field positioner is about 1 dBic but this does not include the feeding system loss which can reduce the realized gain of the entire antenna system. Values around -1 dBic are observed. Given these results and a simulated antenna efficiency of 64%, the total loss for the entire system (feeding system and compact antenna array) can be estimated to be about 1.7 dB (or a 40% total efficiency). Despite these practical concerns, the functionality of the compact feeding circuit has been demonstrated and suitable performance was obtained as a proof of concept.

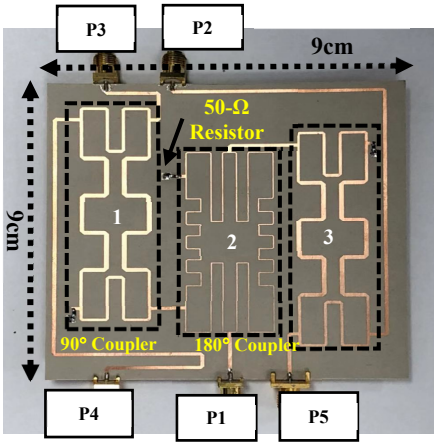

Fig. 6. The fabricated feeding circuit for the array to enable CP radiation. The total dimensions of the passive circuit are 9 cm × 9 cm. Port 1 is the input port, port 2 is a 270° phase delay output, port 3 offers a +/-180° phase delay, port 4 offers a 90° phase delay, and port 5 is a 0° phase delay.

TABLE I. COMPARISON TO OTHER SIMILAR FSP ANTENNAS AND ARRAYS FOUND IN THE LITERATURE CONSIDERING OPTIMIZED (SIMULATED) PARAMETERS

Work	Antenna Type	Number of layers	# of Elements	Design Frequency	Reflection Coefficient	Impedance Bandwidth	Single-Element Size (L × W × H)	Size of the Ground Plane	Realized Peak Gain
[6]	Metallic & PCB	4	2x2 Array	400 MHz	< -10 dB	—	0.05λ × 0.04λ × 0.05λ	0.2λ × 0.2λ	2.6 dBic
[8]	Metallic	4	Single Element	415 MHz	-13 dB	2.9%	0.069λ × 0.065λ × 0.016λ	0.277λ × 0.277λ	-
[9]	Metallic	2	2x2 Array	400 MHz	-34 dB	5%	0.25λ × 0.25λ × 0.05λ	0.67λ × 0.67λ	6.6 dBic
This Work (RT6010LM)	Metallic & PCB	2	2x2 Array	440 MHz	-23 dB	2%	0.056λ × 0.059λ × 0.015λ	0.133λ × 0.133λ	2.1 dBic

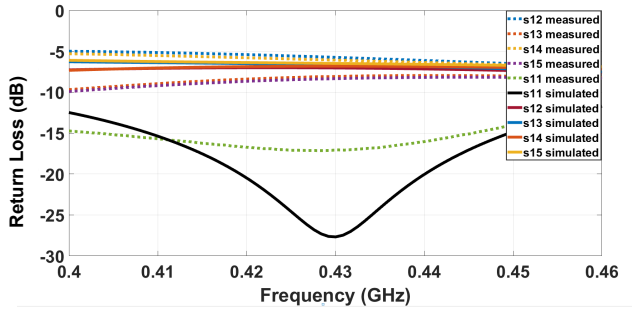

Fig. 7. Measured magnitude of the reflection coefficient (input port) and the transmission coefficient (output port) for the feeding circuit (Fig. 6).

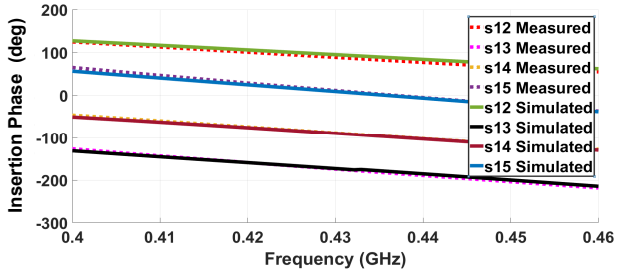

Fig. 8. Measured phase difference in degrees between the input (Port 1) and output (Ports 2, 3, 4 and 5) of the feeding circuit (Fig. 6).

3. ANTENNA ASSEMBLY AND RESULTS

Considering the individual FSPs and the 2 × 2 antenna array arrangement as discussed in Section II, the element spacing and all antenna dimensions were also further optimized using CST. Measured reflection coefficient values are shown in Fig. 9 and are compared to simulations with reference to the antenna inputs. It can be observed that $|S_{ii}|$ is less than -15 dB at 440 MHz for each antenna element. The LHCP realized gain maximum was also about 2 dBic and the antenna efficiency was 64% at 440 MHz for the complete antenna structure without the feeding system loss. Also, the axial ratio was less than 3dB over a 125° beam angle range.

Given these simulated results, the 2×2 sequentially rotated FSP array was then fabricated and measured. All metallic sections for the FSP antenna elements were made by hand soldering and using planar copper plates with a 0.3 mm thickness. The first metallic layers were also soldered to the coaxial probe pins for 50-Ω SMA connectivity at the antenna backside.

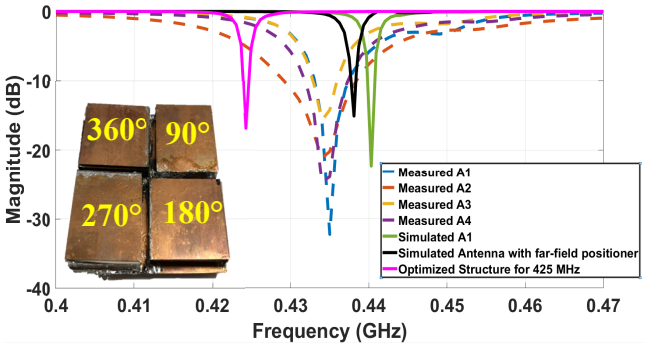

Fig. 9. Measured $|S_{11}|$ at the antenna ports for the fabricated prototype in free space. The simulation model also considers practical fabrication tolerances. Measured dimensions are as follows for all elements: L_{gap} = 2.5 mm, d_u = 1.6 mm, $d_{substrate}$ = 0.635 mm, d_{foam} = 1 mm, L = 43 mm, W = 38 mm, t = 0.3 mm, d = 8.3 mm, and X_f = 3 mm.

Since the assembly of the antenna elements was done by hand, the patch dimensions were not perfectly consistent with the optimized simulation model. For example, dimensional deviations of about 0.5 mm or less were observed (see the captions of Figs. 2 and 9) for the fabricated prototype; i.e. the overall antenna height of the fabricated prototype has been increased from 10 mm to 10.2 mm, while the position of the SMA coaxial feed probes X_f was 3 mm (instead of 2.8 mm originally). Nevertheless, all measured dimensions were imported to the simulation software CST (see Fig. 9). As expected these fabrication inaccuracies slightly altered the resonant frequencies for the individual elements. For example, the proposed antenna design operated at 425 MHz. However, the simulated operating frequency for the fabricated model shifted to 440 MHz.

Fig. 10. Perspective view of the fabricated FSP array.

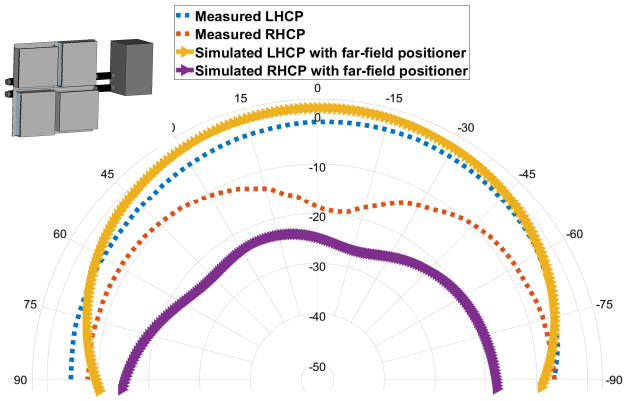

Fig. 11. Measured and simulated beam pattern plots for the compact FSP array. Simulation results include the metallic far-field positioner in the CST simulation model.

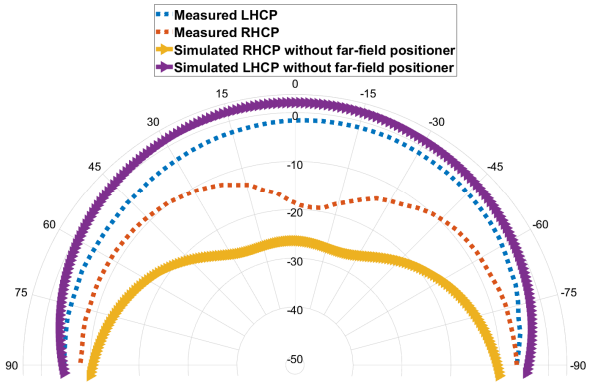

Fig. 12. Measured and simulated beam pattern comparison for the compact FSP array.

The anechoic chamber at Heriot-Watt University and a Keysight N5255A PNA along with a DAMS 7000 far-field positioner were used to measure the array prototype (see Fig. 10, and results in Figs. 10 to 14 and Table II). As observed, when the fabricated antenna dimensions were included in the simulations, as well as the far-field positioner, the matching frequency was shifted by around 3 MHz, providing general agreement with the simulations and measurements. Also, the measured maximum LHCP gain was recorded to be -1.5 dBic and -1.2 dBic (see Figs. 11 and 12) at 0° (broadside) and -22°, respectively, defining a minor beam squint. In addition, the cross-polarization levels (RHCP) are low and reach values which are about 20 dB below the main beam maximum defining the axial ratios which are less than 3 dB from about -40° to +40°.

It should be mentioned that the far-field positioner is defined by a metal and plastic housing and this is the likely cause of the squint in the main beam pattern, resonant frequency shift, and cross-polarization level (RHCP) increase. To accommodate for this, the material properties of the far-field positioner were included in CST (Fig. 11). With this additional modeling of the measurement setup, the simulated beam patterns are better matched to the measurement in terms of the noted squint (see Figs. 11 and 12); i.e. the maximum realized gain appeared at -22˚ for the simulated beam pattern,

TABLE II. ANTENNA RESULTS INCORPORATING THE FEEDING SYSTEM

	Simulated *without* far field positioner (440 MHz)	Simulated *with* far field positioner (437 MHz)	Measured (430 MHz)
Broadside Gain (LHCP)	0.35 dBic	-0.7 dBic	-1.2 dBic
X.Pol. (RHCP)	< 24.5 dBic	< 22 dBic	< 18 dBic
Cone angle in which AR < 3 dB	-65° < θ < +65°	-50° < θ < +50°	-37° < θ < 37°

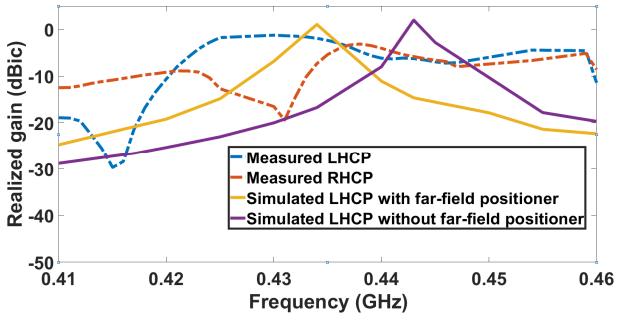

Fig. 13. Measured and simulated realized gain versus frequency for the compact FSP array.

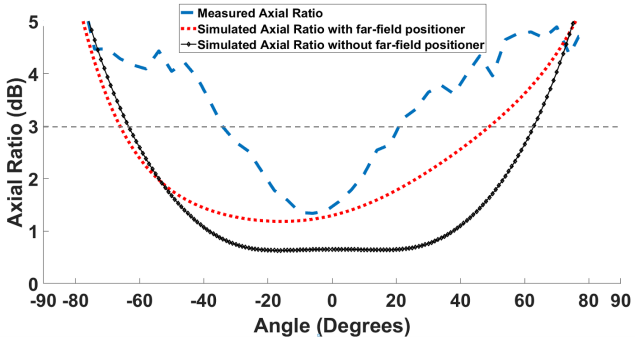

Fig. 14. Measured and simulated axial ratio versus beam angle in the principal plane for the compact FSP array.

while the simulated realized gain has been reduced to 1 dBic at 437 MHz (originally 2.1 dBic at 440 MHz). Considering that the positioner has metallic parts and is in the reactive near-field of the antenna and the noted fabricated dimensions, results are in general agreement with the simulations and provide a good proof of concept for the proposed compact array.

4. CONCLUSIONS

This paper presented a miniaturized folded-shorted patch array by using PCB implementation for operation at the UHF frequency band. Applications for the antenna include placement on CubeSats and other small satellites for telemetry and low data rate communications.

A notable design challenge with the array is the achieved miniaturization within an electrically small volume. In addition, left-handed circular polarization is realized by the inclusion of a compact feeding system connected to the FSP antenna array system for phase quadrature excitation. Moreover, measured cross-polarization values are below -18 dBic and axial ratio values are less than 3 dB from about -40° to +40°. For the fabricated prototype, the physical dimensions of the 2×2 array were $0.129\lambda \times 0.129\lambda \times 0.014\lambda$ for operation at about 430 MHz.

Fabrication and measurement practicalities have also been included in the simulation model, ensuring a close agreement with the measurements. Future work can include 3-D printing technology for such an antenna structure to improve fabrication accuracy while also maintaining antenna efficiency and CP performances.

ACKNOWLEDGEMENT

This work has been partially supported by the EU H2020 Marie Skłodowska-Curie Individual Fellowship #840854 ViSionRF and MSCA-IF 2015 CSA-EU.

REFERENCES

[1] S. Gao, et al., "Antennas for Modern Small Satellites," *IEEE Antennas and Propagation Magazine*, vol. 51, no. 4, pp. 40-56, Aug. 2009.

[2] K. Kan So, H. Wong, K. Man Luk , C. H. Chan, Q. Xue, "A Miniature Circularly Polarization Patch Antenna Using E-Shaped Shorting Strip", *in Proc., 4th EuCAP*, Barcelona, 2010, pp. 1-3.

[3] S. Maci, G. B. Gentili, P. Piazzesi, and C. Salvador, "Dual-band slot loaded patch antenna," *IEEE Proc. Microwaves, Antennas and Propagation*, vol. 142, no. 3, pp. 225–232, Jun. 1995.

[4] H. K. Kan and R. B. Waterhouse, "Size reduction technique for shorted patches," *Electron. Lett.*, vol. 35, pp. 948-949, June 1999.

[5] G. A. Mavridis, D. E. Anagnostou and M. T. Chryssomallis, "Evaluation of the Quality Factor, Q, of Electrically Small Microstrip-Patch Antennas", *IEEE Antennas and Propagation Magazine*, Vol. 53, Is.4, Aug. 2011, pp. 216–224.

[6] S. K. Podilchak, A. P. Murdoch, and Y. M. M. Antar, "Compact Microstrip-Based Folded shorted Patches", *IEEE Antenn. Propagat. Mag.*, pp. 88-95, Apr. 2017.

[7] R. Li, G. DeJean, M. M. Tentzeris, and J. Laskar, "Development and Analysis of a Folded Shorted-Patch Antenna with Reduced Size," *IEEE Trans. Antenn. Propagat.*, vol. 52, no. 2, pp. 555–562, Feb. 2004.

[8] J. Zhang, and O. Berinbjerg, "Miniaturization of multiple layer folded patch antennas", *in Proc., 3rd EUCAP*, pp. 2164 – 3342, 2009.

[9] T. Debogovic, P. Robustillo-Bayon, N. Šaponjić, F. Bongard, M. Sabbadini, F. Tiezzi and J. Mosig, "Low Profile Multi-Function Antenna System for Small Satellites", *in Proc., 10th EUCAP,* 2-June, Switzerland, 2016.

[10] S. K. Podilchak, M. Caillet, D. Lee, Y. M. M. Antar, L. Chu, J. Cain, M. Hammar," Compact Antenna for Microsatellite Using Folded Shorted Patches and Integrated Feeding Network", *IEEE Transactions on Antennas Propagation*, vol. 61, no. 9, pp. 4861-4866, Sept. 2013.

[11] J. Huang, "A technique for an array to generate circular polarization with linearly polarized elements," *IEEE Transactions on Antennas and Propagation*, vol. 34, no. 9, pp. 1113–1124, Sept. 1986.

BIOGRAPHIES

YuePei Li *received the M.Eng. degree in electrical engineering from Heriot-Wat University, U.K., in 2019. He is currently pursuing the Ph.D. degree with the School of Engineering and Physical Sciences, Heriot-Watt University, U.K. His primary research interests include the areas of miniaturized antennas for satellite communication and wireless authentication through radio frequency fingerprinting.*

Symon K. Podilchak *received the B.A.Sc. degree in Engineering Science from the University of Toronto, ON, Canada, in 2005, the M.A.Sc. and the Ph.D. degrees in Electrical Engineering from Queen's University, Kingston, ON, Canada, in 2008 and 2013, respectively, where he was an Assistant Professor, from 2013 to 2015. He then joined Heriot-Watt University, Edinburgh U.K., in 2015, as an Assistant Professor, and became an Associate Professor, in 2017. His research was supported by the H2020 Marie Skłodowska-Curie European Research Fellowship. He currently serves as a Lecturer with the European School of Antennas. He is also a Senior Lecturer with The University of Edinburgh, School of Engineering.*

Dr. Podilchak is a Registered Professional Engineer (P.Eng.). He has had industrial experience as a computer programmer and designed 24 and 77 GHz automotive radar

systems with Samsung and Magna Electronics. Recent industry experience also includes the design of high frequency surface wave radar systems, professional software design, and implementation for measurements in anechoic chambers with the Canadian Department, National Defence and the SLOWPOKE Nuclear Reactor Facility. He has also designed new compact multiple-input–multiple-output (MIMO) antennas for wideband military communications and highly compact circularly polarized antennas for microsatellites with COM DEV International, and new wireless power transmission with Samsung. His research interests include surface waves, leaky-wave antennas, metasurfaces, UWB antennas, phased arrays, and CMOS integrated circuits.

Dr. Podilchak was a recipient of many best paper awards and scholarships; most notably research fellowships from the IEEE Antennas and Propagation Society and the IEEE Microwave Theory and Techniques Society. He has received the Outstanding Dissertation Award for the Ph.D. degree from Queen's University. He also received a Postdoctoral Fellowship from the Natural Sciences and Engineering Research Council of Canada (NSERC) and four Young Scientist Awards from the International Union of Radio Science (URSI). In 2011 and 2013, he received the Student Paper Award from the IEEE International Symposium on Antennas and Propagation, the Best Paper Prize for Antenna Design from the European Conference on Antennas and Propagation for his work on CubeSat antennas, in 2012, and the European Microwave Prize for his research on surface waves and leaky-wave antennas, in 2016. He was bestowed a Visiting Professorship Award from Sapienza University of Rome, in 2017 and 2019. He was also the Founder and the First Chairman of the IEEE Antennas and Propagation Society and the IEEE Microwave Theory and Techniques Society Joint Chapter of the IEEE Kingston Section in Canada as well as Scotland. In recognition of these services, he has received the Outstanding Volunteer Award from the IEEE, in 2015. He is an Associate Editor of the journal IET Electronic Letters. He was recognized as an Outstanding Reviewer of the IEEE Transactions on Antennas and Propagation by the IEEE Antennas and Propagation Society, in 2014.

Dimitris E. Anagnostou (S'98–M'05–SM'10) received the B.S.E.E. degree from the Democritus University of Thrace, Greece, in 2000, and the M.S.E.E. and Ph.D. degrees from the University of New Mexico, Albuquerque, NM, in 2002 and 2005, respectively. From 2005 to 2006, he was a Postdoctoral Fellow with the Georgia Institute of Technology, Atlanta, GA. In 2007, he joined as Assistant Professor the SD School of Mines & Technology, SD, USA, where he was promoted to Associate Professor with tenure. In 2016, he joined the Heriot Watt University, Institute of Signals, Sensors and Systems (ISSS), Edinburgh, UK, where he is currently an Associate Professor, supported by a Marie Skłodowska-Curie Individual Fellowship. He has also worked at the Kirtland AFB, NM in 2011 as an AFRL Summer Faculty Fellow, and at the Democritus Univ. of Thrace, Greece as Assistant Professor.

He has authored or coauthored more than 150 peer-reviewed journal and conference publications and holds two U.S. patents. His research interests include: reconfigurable antennas applications for space satellites, defense, assisted living and consumer electronics. Research includes also microwave circuits and packaging, radar, phase-change (functional) materials such as VO_2 for reconfigurable electronics and metasurfaces, direct-write, RF-MEMS, sensors, and applications of artificial neural networks, deep learning and machine learning in electromagnetics and health care.

Dr. Anagnostou serves or has served as Associate Editor for the IEEE TRANSACTIONS ON ANTENNAS AND PROPAGATION (2010-2016) and the IET MICROWAVES, ANTENNAS AND PROPAGATION (since 2015). He was Guest Editor for two IEEE ANTENNAS AND WIRELESS PROPAGATION LETTERS Special Clusters. He is a member of the IEEE AP-S Educational Committee, and of the Technical Program Committee (TPC) of the IEEE AP-S International Symposia. He is also a reviewer for Nature, IEEE Transactions, and other international journals. He received the 2010 IEEE John D. Kraus Antenna Award, the 2011 DARPA Young Faculty Award by the U.S. Department of Defense, the 2014 Campus Star Award by the American Society for Engineering Education (ASEE), the 2017 Young Alumni Award by the University of New Mexico, four Honored Faculty Awards by SDSMT, and the H2020 Marie Skłodowska-Curie Individual Fellowship. His students have also been recognized with IEEE and university awards (Engineering Prize, HWU, Best PhD Thesis, SDSMT, and other). He is a member of HKN Honor Society, ASEE, and of the Technical Chamber of Greece as a registered Professional Engineer (PE).